Article

Easy-preparable butyrylcholinesterase/microgel construct for facilitated organophosphate biosensing

Larisa V. Sigolaeva, Snezhana Yu. Gladyr, Olga Mergel, Arjan P.H. Gelissen, Michael Noyong, Ulrich Simon, Dmitry V. Pergushov, Ilya N. Kurochkin, Felix A. Plamper, and Walter Richtering

Anal. Chem., **Just Accepted Manuscript** • Publication Date (Web): 03 May 2017

Easy-preparable butyrylcholinesterase/microgel construct for facilitated organophosphate biosensing

Larisa V. Sigolaeva[a*], Snezhana Yu. Gladyr[a], Olga Mergel[b], Arjan P.H. Gelissen[b], Michael Noyong[c], Ulrich Simon[c], Dmitry V. Pergushov[a], Ilya N. Kurochkin[a], Felix A. Plamper[b], Walter Richtering[b]

[a] *Department of Chemistry, M.V. Lomonosov Moscow State University, 119991 Moscow, Russia*
[b] *Institute of Physical Chemistry II, RWTH Aachen University, 52056 Aachen, Germany*
[c] *Institute of Inorganic Chemistry, RWTH Aachen University, 52074 Aachen, Germany*

**corresponding author:*
Larisa V. Sigolaeva, lsigolaeva@genebee.msu.ru

Abstract

A versatile guest matrix was fabricated from a temperature- and pH-sensitive poly(*N*-isopropylacrylamide)-*co*-(3-(*N*,*N*-dimethylamino)propylmethacrylamide) microgel (poly(NIPAM-*co*-DMAPMA, MG) for the gentle incorporation of butyrylcholinesterase (BChE). The microgel/BChE films were built up on a surface of graphite-based screen-printed electrodes (SPEs) premodified with MnO_2 nanoparticles via a two-step sequential adsorption under careful temperature and pH control. Due to that, a rather simple amperometric biosensor construct was formed, which uses butyrylthiocholine as BChE substrate with following MnO_2-mediated thiocholine oxidation at a graphite-based SPE. The complexation of BChE with the microgel was found to be safe and effective as confirmed by a high operational and rather good long-term storage stability of the resultant SPE-MnO_2/MG/BChE biosensors. The small mesh size of the microgel with respect to the size of BChE results in a predominant outer complexation of BChE

within the dangling chains of the microgel rather than a deep penetration of the enzyme into the microgels. Due to such surface localization, BChE is easily accessible both for the substrate and for cholinesterase inhibitors. This was supported by the analytical characteristics of the SPE-MnO_2/MG/BChE biosensor that were examined and optimized both for the substrate and for the enzyme detection. The SPE-MnO_2/MG/BChE biosensor enabled precision detection of organophosphorus pesticides (diazinon(oxon), chlorpyrifos(oxon)) in aqueous samples with minimized interference from extraneous (non-analyte) substances (e.g., ions of heavy metals). The detection limits for diazinon(oxon) and chlorpyrifos(oxon) were estimated to be as low as 6×10^{-12} M and 8×10^{-12} M, respectively, after 20 min preincubation with these irreversible inhibitors of BChE.

Keywords: microgel, *N*-isopropylacrylamide, poly(*N*-isopropylacrylamide)-*co*-(3-(*N*,*N*,-dimethylamino)propylmethacrylamide), stimuli-sensitivity, adsorption, enzyme immobilization, butyrylcholinesterase, surface modification, thin films, organophosphorus compounds, biosensor, pesticide detection

Introduction

The interest for environmental monitoring represents an urgent issue because of the expanding exposure of chemicals in daily life. Organophosphorus compounds (OPs), the main representatives of which include pesticides, nerve agents, natural toxins, and some drugs,[1,2] are a big family of highly toxic environmental pollutants. The high toxicity of OPs to humans results from their fast and irreversible interaction with multiple target enzymes. These enzymes include primary targets, e.g., acetylcholinesterase (AChE, acute cholinergic toxicity) and neuropathy target esterase (NTE, delayed neuropathy); as well as secondary targets, e.g., butyrylcholinesterase (BChE) and carboxylesterase (CaE), which act as scavengers of OPs,[3-5] while paraoxonase (PON1) can hydrolyze and detoxify OPs. Surveillance of living organisms exposed to cholinergic and neuropathic OPs depends on the toxicity of a specific OP, its dose, and the individual sensitivity to OPs.[6]

Defending against such agents requires rapid, sensitive, and specific detection as well as quantification of OPs in environmental matrices preferably before contact and following toxic exposure to humans. Enzymatic biosensors represent ideally suited prescreening tools for rapid and simple express analysis of OPs pollutants. Moreover, the same enzymes, AChE or BChE, are widely used as a recognition element in biosensors for OPs detection. Numerous and various constructs of AChE/BChE biosensors have been reported since 1980s till nowadays.[7-9] However, problems appear frequently, which are the high number of steps required for the preparation and measurement procedures, the instability of the response and short life-times. Therefore, the development of advanced AChE/BChE constructs, especially those suitable for large-scale production and in-field application is of a permanent continuing relevance.

The performance of cholinesterase biosensors is very dependent on the methods used for enzyme immobilization. Currently, chemical covalent bonding and cross-linking as well as encapsulation and physical entrapment processes are the most popular methods for the enzyme immobilization.[8] However, these methods can cause structural deformation/deterioration of the

enzyme or introduce steric hindrance to the catalytic sites, leading to a reduction in enzymatic activity.[7]

Microgels exhibit combined properties of very different classes of materials, like colloidal, polymeric, and surfactant systems[10] that enables novel applications in very different fields, like, e.g., sensors[11-13], catalysis[14,15] and separation technologies[16]. Microgels are typically prepared through precipitation polymerization, by which they can be synthesized on a large scale, with good particle size control, mesh size control, and relatively facile functionalization.[17,18] It is possible to synthesize charged microgels by adding a functional (ionic) comonomer during the synthesis.[19] More complex core-shell microgel structures are intensively developed as well.[20-23] Microgels like hydrogels can be considered as perfect host matrices for biomolecules, providing an excellent biocompatible environment to preserve their active and functional structure.[24]

Stimuli-responsive properties are a special feature of (micro)gels based on poly(*N*-isopropylacrylamide) PNIPAM, possessing a classical lower critical solution temperature, LCST, behavior in aqueous solutions.[25] The collapse of the PNIPAM gels is accompanied by expelling water from its interior over a narrow temperature range usually referred to as the volume phase transition temperature (VPTT).[26] A decrease of the temperature below VPTT induces reversible (micro)gel swelling to its initial volume. As soon as charged moieties are present in the polymer, charged polymer networks can absorb more water compared to uncharged ones.[27,28] By that, the temperature-induced collapse of PNIPAM-based (micro)gels can be either less pronounced or even suppressed.[29]

Our former experience with temperature- and pH-sensitive poly(*N*-isopropylacrylamide)-*co*-(3-(*N*,*N*-dimethylamino)propylmethacrylamide) microgel (poly(NIPAM-*co*-DMAPMA MG) results in a novel simple and fast strategy for physical entrapment of biomolecules by the polymeric matrix, this physical entrapment being non-destructive and enzyme friendly. In particular, it was demonstrated that by temperature-induced stimulation of both microgel

adsorption and enzyme loading, we can effectively control the amount of the microgel adsorbed on a hydrophobic interface as well as the amount and the spatial localization of the enzyme interacting with the microgel film.[30] Enzyme molecules can or cannot penetrate into the microgel interior depending on the ratio of biomolecule size to the microgel mesh size. For instance, small choline oxidase (M = 72 kDa) can be localized mainly inside microgel particles while butyrylcholinesterase (M = 440 kDa (tetramer) with four equal subunits of 110 kDa) locates only outside the microgel particles, correspondingly.[31]

In this work, we focus on a description of a very simple and stable MG/BChE biosensor construct. This amperometric biosensor uses butyrylthiocholine as BChE substrate with following MnO_2-mediated thiocholine oxidation at a graphite-based screen-printed electrode (SPE). In spite of the non-covalent physical binding of BChE to the microgel, a rather strong interaction of the enzyme with the cross-linked polymer matrix was found that results in a long-term stability of the enzymatic response measured for immobilized large multi-subunit BChE localized predominantly in the outer layer of the microgel. Therefore, we consider microgels as a perfect host matrix for biocatalysts, providing structure and function maintaining, highly hydrated, and non-denaturing environment to preserve the active and functional biostructure. Due to mainly surface localization, BChE is easily accessible both for the substrate and for cholinesterase inhibitors, providing high sensitive and fast OPs detection in aqueous samples. To the best of our knowledge, this is a first example of a BChE biosensor for OPs detection that was designed with a microgel matrix. The fabrication method, measuring principle, and the arrangement of the active biosensing coating for the MG/BChE biosensor are summarized in Scheme 1.

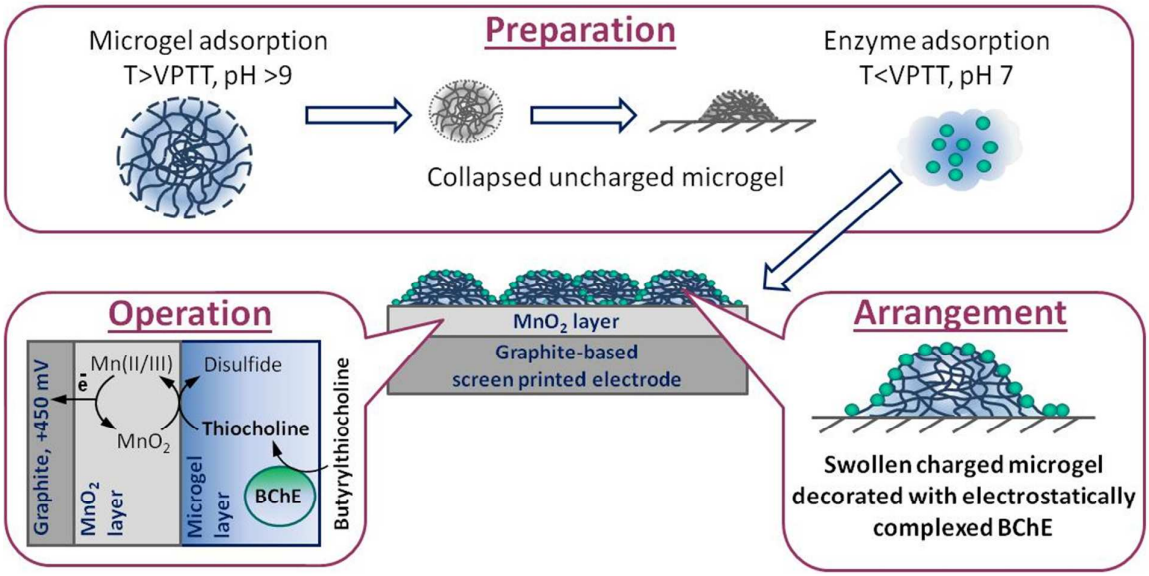

Scheme 1. The fabrication method, measuring principle, and the arrangement of the active biosensing coating for the MG/BChE amperometric biosensor.

Experimental Part

Materials

Butyrylcholinesterase (BChE) from equine serum, E.C. 3.1.1.8, activity 1390 U/mg of protein, S-butyrylthiocholine chloride (BTCh), diazinon, chlorpyrifos, HEPES (4-(2-hydroxyethyl)piperazine-1-ethanesulfonic acid, sodium salt), and liquid bromine were purchased from Sigma-Aldrich. The poly(NIPAM-*co*-DMAPMA) microgel was synthesized by precipitation polymerization according to the procedure, described in detail in a reference.[30] Tris (tris(hydroxymethyl)aminomethane) buffer solutions (10 mM Tris) with pH of 7.0 or 9.0 were prepared by mixing stock solutions of 10 mM Tris and 10 mM Tris-HCl (Tris and Tris-HCl were obtained from Sigma-Aldrich). All other chemicals (ascorbic acid and inorganic salts) were of analytical grade and used without further purification. All aqueous solutions were prepared using deionized water (18.2 MΩ cm).

Methods

Microgel/enzyme film assembly. For an electrochemical enzymatic response assay of the microgel/enzyme films, the SPEs were fabricated on poly(vinyl chloride) substrates of 0.2 mm thickness by means of conductive graphite paste (Gwent, UK) screen-printed by a semiautomated Winon machine (model WSC-160B, China) with a 200 mesh screen stencil. Each SPE consisted of a round-shaped working area (2.5 mm diameter), a conductive track, and a square extremity for the electrical contact. Before adsorption of the microgel and the enzyme, all SPEs were premodified by a peroxide-sensitive MnO_2 layer according to a published protocol (for details see also SI).[32] The MnO_2-modified SPEs were stored dry at ambient temperature until further use.

Microgel particles were adsorbed onto SPE/MnO_2 at 60°C by dipping the SPE/MnO_2 into a preheated dispersion of poly(NIPAM-*co*-DMAPMA) microgel at a concentration of 1 g/L in 10 mM Tris of pH 9.0 and incubating them for 40 min. After incubation, the surface was rinsed with

Milli-Q water at the same temperature at which adsorption was carried out and then was very shortly (for 1–2 seconds) blown by a stream of warm air. Directly after this, BChE was adsorbed in a similar way at 25°C for 10 min from aqueous solutions in 10 mM Tris of pH 7.0 with specified concentrations, followed by rinsing with Milli-Q water and short drying with a stream of air. To prevent a loss of enzymatic activity, the SPEs covered by microgel/enzyme films were stored at +4°C until further use.

Electrochemical assay of enzymatic responses. Electrochemical experiments were performed at ambient temperature in a one-compartment electrochemical cell under stirring (volume of 1 ml) using a two electrode configuration. The SPE covered by microgel/enzyme film with an active surface area of 0.049 cm^2 served as the working electrode and Ag/AgCl (with a surface area of 1.03 cm^2) was used as a counter/reference electrode. A micro-potentiostat IPC-Micro (Kronas Ltd., Russia) used for electrochemical measurements was connected to a computer and electrochemical parameters were controlled by using the micro-potentiostat software. The measurements were carried out in 50 mM HEPES buffer with 30 mM KCl (pH 7.5). BTCh was used for the measurement of the sensor response of SPE/MnO_2/MG/BChE constructs at an applied potential of +450 mV *vs.* Ag/AgCl reference electrode. The analytical signal of the electrode was determined as a value of the steady-state baseline current change (the difference between an average value of steady-state baseline current before and after substrate addition). Each electrochemical result is presented as mean ± SD calculated from at least three sensor responses obtained for at least three different electrodes.

Inhibitors assay. Diazinon or chlorpyrifos, preliminarily oxidized with bromine water to its oxone form, which is a more efficient inhibitor of BChE, were used as test inhibitors. Bromine water was prepared by the addition of 4 μL bromine to 12.5 mL of 0.5 M KBr. Diazinon or chlorpyrifos stock solutions were oxidized during 3 min and then diluted with 50 mM HEPES buffer with 30 mM KCl (pH 7.5) to the final concentrations in a range of 0 – 10 nM. A SPE-MnO_2/MG/BChE sensor was prepared using 2.5×10^{-8} M BChE stock solution and the initial

sensor response was measured for 1 mM of BTCh (A_0). Then, the SPE-MnO_2/MG/BChE sensor was incubated in a solution containing a specified concentration of the OP inhibitor for a specified time period (2-60 min). After a short washing step, the residual sensor response was measured for 1 mM of BTCh (A_i). Inhibition curves were presented as the relative sensor responses ($A_i/A_0 \times 100\%$).

Results and Discussion

Fabrication process and surface characterization

As we reported earlier[30,31] the pH- and thermo-responsive behavior of the poly(NIPAM-*co*-DMAPMA) microgel allows controlling the amounts of the adsorbed microgel and enzyme in the process of biosensor fabrication. The MG/BChE films were formed on a surface of graphite-based SPEs premodified with MnO_2 nanoparticles via a two-step sequential adsorption under careful temperature and pH control. To facilitate the adsorption of microgels onto the hydrophobic surface (here onto graphite-based SPE, premodified with MnO_2 nanoparticles serving as mediator for the oxidation of H_2O_2), it is necessary to use high pH values (pH=9.0) and elevated temperatures (50-60ºC), such that the microgel is in its non-charged, deswollen and rather hydrophobic state. After short washing with water and blow-off with an air stream, the microgel-modified surface is ready for the second modification stage: the adsorption of enzyme. Obviously, one should carry out adsorption of BChE under conditions when the enzyme is oppositely charged to the microgel[30,31] to ensure their electrostatically-driven interaction. We consider pH=7.0 as an optimum as the microgel bears positive charges while BChE having an isoelectric point (IEP) of 4.3[31] possesses negative charge. As found earlier,[31] the small mesh size of the poly(NIPAM-*co*-DMAPMA) microgel[33,34] with respect to the size of active BChE in its tetrameric form results in outer complexation of the enzyme in the periphery of the microgel particles rather than inner penetration into them. Due to this, a rather simple amperometric

biosensor construct was formed, which uses BTCh as a substrate for BChE, with following MnO_2-mediated thiocholine oxidation at a graphite-based SPE (Scheme 1).

To visualize the process of biosensor preparation, we firstly examined the film morphology by scanning electron microscopy (SEM). A highly rough and hydrophobic surface of bare graphite-based SPE represents a layer of uniformly distributed large flakes covered by a non-uniform thin film of small flakes (Figure S-1A). The modification of a naked SPE with MnO_2 sol solution does not induce any notable changes in film morphology that is in line with our former results.[32,35]

The following adsorption of poly(NIPAM-*co*-DMAPMA) microgels leads to the appearance of numerous spherical objects with a diameter of about 70-90 nm, which one can presumably attribute to individual microgel particles in the dry state (Figure S-1B). The further adsorption of BChE results in slight smoothing of the relief (Figure S-1C), although the resolution of the SEM is not sufficient to see individual globules of the enzyme.

The films of the poly(NIPAM-*co*-DMAPMA) microgel alone as well as the films of the microgel interacted with BChE were deposited under the same conditions onto a surface of highly oriented pyrolytic graphite (HOPG) and were additionally imaged (in dry state) by atomic force microscopy (AFM). As seen from the distinct and detailed AFM phase images (Figure S-2), the film of intact microgel appears as randomly distributed individual objects (microgel particles) of a pancake shape surrounded by dangling chains (Figure S-2A). They are characterized by a rather smooth surface. This observation is similar to our previous data[30,36] and also to other reports.[37,38] The interaction of the microgel film with BChE leads to considerable changes of the AFM phase image. All microgels including their dangling chains are covered by a layer of adsorbed BChE. It appears like numerous small spherical objects found in a detailed AFM phase image (Figure S-2B and also images in our previous publication[31]) and confirms the successful enzyme binding.

Analytical characteristics of BTCh and BChE detection

Using the above described approach, a very simple amperometric SPE-MnO_2/MG/BChE biosensor construct was formed, wherein BChE is physically entrapped by the outer layer of microgels, being well-accessible for the substrate and for the inhibitor as well. The measuring principle of the sensor is based on the application of BTCh as a BChE substrate. The enzymatic hydrolysis of this substrate leads to an accumulation of electrochemically active thiocholine, while the following MnO_2-mediated thiocholine oxidation at the graphite-based SPE results in a generation of a current that was measured amperometrically. A detailed description of the process of MnO_2-mediated thiocholine detection can be found elsewhere.[35] We used optimum operational parameters for the thiocholine detection that were recommended[35] and examined the analytical characteristics of the new SPE-MnO_2/MG/BChE biosensor.

The change in sensor responses (a steady-state current) registered by the SPE-MnO_2/MG/BChE sensor as a function of the BTCh concentration is shown in Figure 1A with the initial part of the substrate calibration curve being given in Figure 1A, Inset. The calibration curve exhibited linearity in the range of 0.1 μM - 0.2 mM for BTCh with the regression coefficients of 0.996. The detection limit (DL) for BTCh was calculated using S/N (signal-to-noise ratio) = 3 criterion and was found to be 0.1 μM that is considerably lower than reported before for BChE biosensors with a 7,7′,8,8′-tetracyanoquinodimethane- or Prussian Blue-mediated thiocholine detection.[39-42] Furthermore, the sensitivity of the BTCh detection was determined to be 84.5 $A \times M^{-1} \times cm^{-2}$. The saturation of the BTCh calibration curve at BTCh concentrations >1 mM additionally allows us to estimate the K_M^{app} value for the enzymatic hydrolysis of BTCh by BChE as 0.27 ± 0.02 that is close to K_M^{app} value of 0.199 ± 0.024 reported for soluble BChE.[43] Based on the substrate calibration curve (Figure 1A), the BTCh concentration of 1 mM (close to saturation of the substrate calibration curve) was chosen as an optimum for all further experiments.

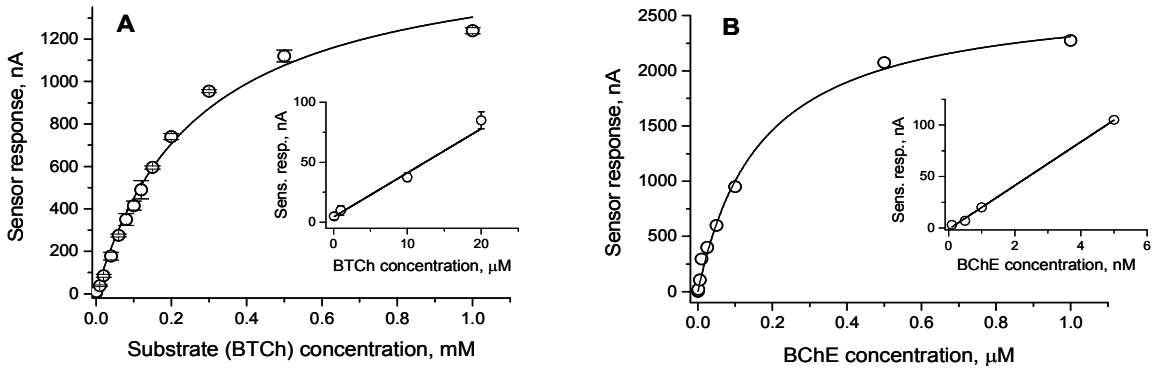

Figure 1. (A): Dedependence of steady-state current on the BTCh concentration for SPE-MnO_2/MG/BChE sensor. Inset: the initial part of the substrate calibration curve. Conditions: 50 mM HEPES with 30 mM KCl, pH 7.5; room temperature; SPE-MnO_2/MG/BChE sensor was prepared at 1 μM BChE concentration; data represents Mean Values ± SD (n = 3). (B): Dependence of steady-state current for SPE-MnO_2/MG/BChE sensor on the BChE concentration that was used for sensor preparation. Inset: the initial part of the curve. Conditions: 1 mM of BTCh in 50 mM HEPES with 30 mM KCl, pH 7.5, room temperature.

The effect of the sensor response on the BChE concentration taken for the sensor preparation was examined as well. Figure 1B shows the analytical calibration curve of the proposed biosensor for BChE with the initial part of the calibration curve being given in Figure 1B, Inset. The calibration curve exhibited linearity in the range of 0.1 nM - 100 nM. The DL for BChE determined at S/N = 3 criterion was equal to 0.1 nM. Based on this dependence (Figure 1B), we choose a concentration of BChE of 2.5×10^{-8} M, which is within the linearity, as an optimum one for the sensor preparation. The sensors prepared with this optimum BChE concentration show a well-measurable and a well-reproducible analytical response (of about 300 nA) at the minimum enzyme amount consumed for sensor preparation. The latter seems to be important for large-scale manufacturing of cheap disposable sensors intended for single measurements.

Reproducibility, repeatability, stability of biosensors

Prepared at the optimal condition (2.5×10^{-8} M of BChE), the SPE-MnO_2/MG/BChE biosensors were further examined for the reproducibility, repeatability, and stability of the analytical responses.

The reproducibility of the sensor preparation (or manufacturability) was tested for a large group of similarly prepared electrodes measured under standard conditions. The resultant SPE-MnO_2/MG/BChE biosensor exhibited very good manufacturability with coefficient of variation, CV, of 12% for 70 sensors prepared (Figure S-3).

The repeatability and operational stability of SPE-MnO_2/MG/BChE biosensors was examined by repeated measurements of a standard analyte concentration (1 mM of BTCh) for a single sensor (Figure 2A). One can see that SPE-MnO_2/MG/BChE biosensor demonstrates stable and rather reproducible responses. The repeatability of sensor response was calculated as CV for 15 repeated measurements at the standard analyte concentration and was found to be of 3%. The operational stability can be characterized quantitatively as a percentage of the sensor response change per single measurement and can be calculated according to the formula: $\Delta I = 100\% \times tgI/I_1$, where tgI is the slope of the dependence of the analytical signal on the number of repeated measurements (Figure 2A) normalized to the initial analytical signal I_1 and given as a percentage. Calculated by this way, ΔI value for SPE-MnO_2/MG/BChE sensors was found to be -0.34 ± 0.02.

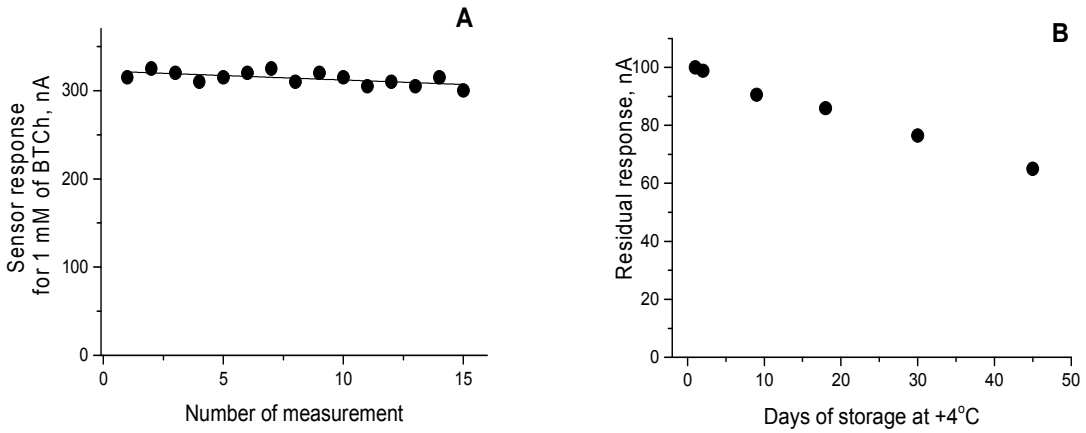

Figure 2. The analytical responses of SPE-MnO_2/MG/BChE biosensor for 15 repeated additions of 1 mM of BTCh (A); the analytical responses of SPE-MnO_2/MG/BChE biosensors measured after storage in dry state refrigerated at +4°C (B). All biosensors were prepared at 2.5×10^{-8} M of BChE concentration and examined for analytical response to 1 mM of BTCh in 50 mM HEPES with 30 mM KCl, pH 7.5, room temperature.

We have further evaluated the storage stability of the dried biosensors at +4ºC (Figure 2B). Tests showed that despite the response of these sensors to 1 mM of BTCh decreases gradually with time, they, nevertheless, still kept 65% of initial activity for 45 days of storage.

Thus, SPE-MnO_2/MG/BChE sensors demonstrate fast stable and reliable responses and are characterized by a high operational stability and a rather good long-term storage stability. These analytical characteristics indicate that these new sensors perfectly suit the purpose of monitoring BChE inhibitors.

Pesticide detection

The irreversible inhibition of cholinesterases (AChE and BChE) by OPs is the basis of a quantitative (biosensor) assay of these toxic cholinesterase inhibitors. When the analyte is not present in the solution, the substrate (BTCh in our case) is converted into thiocholine and butyric acid. The following thiocholine oxidation by the applied voltage produces the initial analytical response (A_0). Preincubation with an inhibitor followed by conversion of the substrate decreases the analytical response or makes it even null (A_i). Obviously, the analytical response is inversely proportional to the concentration of inhibitor in the analyte and the exposed preincubation time as well.

To demonstrate the potential of the SPE-MnO_2/MG/BChE biosensor for inhibitor analysis, we examined two OPs, diazinon and chlorpyrifos, which are included in the Norman list of emerging substances (http://www.norman-network.net/). Both are rather frequently used as a main active ingredient of domestic insecticides. After exposure to the living body, each of these pesticides firstly methabolically converts from the thion (P=S) form to the much more toxic oxon (P=O) derivative and then irreversibly inhibits target enzymes. In our *in vitro* experiments, prior to inhibition tests, each organoposphate was converted from the thion (P=S) form to the more toxic oxon (P=O) form via chemical oxidation by bromine.

The inhibition effects on the SPE-MnO_2/MG/BChE biosensor responses was then examined for different OP concentrations in a concentration range of 0 – 10 nM for a number of preincubation times in a range of 2 – 60 min. Figure 3A shows the inhibition kinetics for diazinon(oxon). It can be seen that the relative sensor response (A_i/A_0*100%) decreases with increasing diazinon(oxon) concentration in the preincubation mixture. The inhibition proceeds very quickly and reaches a plateau level after about 20 min. Therefore, an incubation time of 20 min can be chosen as the best compromise between sensitivity and incubation time and can be selected for the calibration curve for a quantification of the diazinon(oxon) concentration (Figure 3A, Inset). The same is valid for chlorpyrifos(oxon) (Figure 3B). The lower DL defined as an OP concentration that causes 10% inhibition for 20 min of preincubation was found to be 6×10^{-12} M and 8×10^{-12} M for diazinon(oxon) and chlorpyrifos(oxon), respectively. These very low values of DLs obtained are among the lowest DLs reported so far for diazinon or chlorpyrifos detection by the other ChE electrochemical biosensors (Table 1) and they are much lower than the maximum permissible concentrations that set, for example, for drinking water in a range of 10–50 nM for these pesticides.[44]

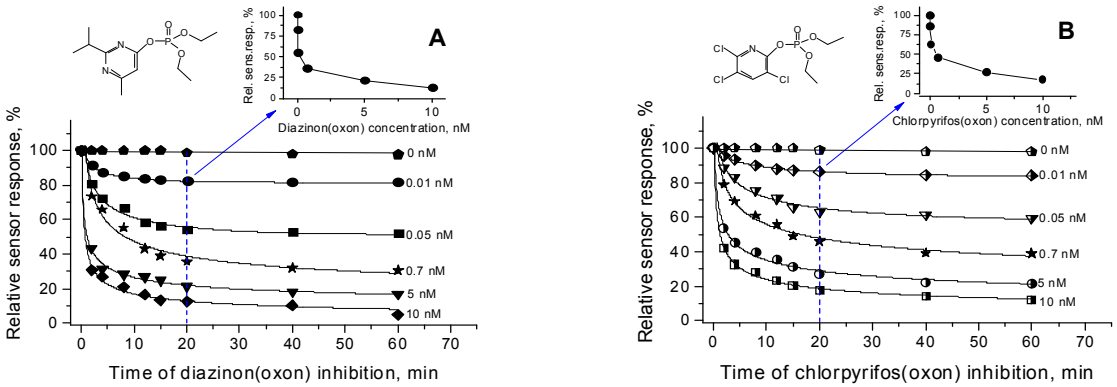

Figure 3. Dependence of the relative sensor response on the time of pre-incubation of SPE-MnO_2/MG/BChE sensor with diazinon(oxon) (A) or chlorpyrifos(oxon) (B). Insets: 20-min calibration curve for inhibitor detection with SPE-MnO_2/MG/BChE sensor. Conditions: response for 1 mM of BTCh in 50 mM HEPES with 30 mM KCl, pH 7.5, room temperature.

Table 1. Comparison of the analytical performance of the SPE-MnO_2/MG/BChE biosensor with some of the ChE electrochemical biosensors applied to the assay of the same analytes.

Analyte	Electrode type	Limit of detection, nM (electrochemical method)	Concentration range, nM	Inhibition time, min	Storage stability, days	Ref.
Diazinon	EpoxyCPE/BChE-CNM	1.5 (amperometry)	1.5–150	10 min	-	[45]
	Pt/(AChE-F127M)-(ChO-F127M)	1.2 (amperometry)	1–100	15 min	80 days	[46]
	Au/MBT/PANI/AChE/PVA	0.6 (amperometry in 98% acetone) 0.48 (amperometry in 98% ethanol)	-	20	-	[47]
	GCE/DEN(PtNPs)/CNT/AChE-ChO-POD	0.17 (CV)	0.17–35	Simultaneously with substrate	Stable signal for at least 20 CV scans	[48]
	SPE-MnO_2/MG/BChE	**0.006 (amperometry)**	**0.006–10**	**20 min**	**65% after 45 days at +4°C**	**This work**
Chlorpyrifos	CPE/MWCNT/AChE[BMIM][BF4]	4	10–1000	15 min	95% after one week at +4°C	[49]
	TCNQ-SPE/AChE	1.2 (amperometry)	Up to 200	10 min	98.4% after 50 days	[50]
	GCE/CHIT/HAuNs/AChE	0.18 (CV/EIS)	0.3–450	10	-	[51]
	GCE/GR-AuNPs/CLDH-AChE	0.15 (DPV)	0.15–410	10 min	89% after 30 days at +4°C	[52]
	Au/MWCNTs-SnO_2-CHIT/AChE/NF	0.15 (DPV)	0.15–270000	14 min	-	[53]
	ITO-glass/cMWCNTs/AChE-Fe_3O_4NPs	0.1 (DPV)	0.1–4	10 min	40% after 90 days at +4°C	[54]
	SPE/PEDOT/AChE-PVA-SbQ	0.01	0.02–10	10 min	Stable signal for at least 10 measurements	[55]
	Au/ss-DNA-SWCNT/PANI/AChE	0.001 (SWV)	0.01–1000	15 min	86% after 5 days at +4°C	[56]
	GCE/SiO_2 nanosheet/AChE-CHIT/NF	0.0005 (amperometry)	0.001–0.1	-	89% after 30 days at +4°C	[57]
	BDD/AuNP-CSs/AChE	0.00013 (DPV)	0.00013–1000	10 min	84.72% after 30 days at +4°C -	[58]
	GCE/AgNPs–cGR–NF/AChE–CHIT/NF	0.000053 M (DPV)	0.0001–10	6 min	88% after 30 days at +4°C	[59]
	SPE-MnO_2/MG/BChE	**0.008 (amperometry)**	**0.008–10**	**20 min**	**65% after 45 days at +4°C**	**This work**

Alphabetical list of abbreviations: AChE – acetylcholinesterase; AgNPs – silver nanoparticles; AuNPs – gold nanoparticles; BDD – boron doped diamond electrode; [BMIM][BF4] - 1-butyl-3-methylimidazolium tetrafluoroborate; cGR - carbonized graphene; CHIT – chitosan; ChE – cholinesterase; ChO – choline oxidase; CLDH - calcined layered double hydroxide; cMWCNTs – carbonized multi-walled carbon nanotubes; CNM – cellulose nitrate membrane; CNT – carbon nanotubes; CPE – carbon paste electrode; CSs – carbon spheres; CV – cyclic voltammetry; DEN - poly(amido amine) dendrimer; DPV - differential pulse voltammetry; EIS - electrochemical impedance spectroscopy; EpoxyCPE – epoxide resin carbon paste electrode; F127M - hybrid mesoporous membrane based on Pluronic F127; Fe_3O_4NPs - Fe_3O_4 nanoparticles; GCE - glassy carbon electrode; GR – graphene; HAuNs – hollow gold nanospheres; ITO – indium tin oxide; MBT – mercaptobenzothiazole; MWCNTs – multi-walled carbon nanotubes; NF – Nafion; PANI – polyaniline; PEDOT - poly(3,4-ethylenedioxythiophene); POD – peroxidase; PtNPs – platinum nanoparticles; PVA – polyvinyl acetate; PVA-SbQ - polyvinyl alcohol functionalized with methyl pyridinium methyl sulfate; SnO_2 – tin oxide nanoparticles; ss-DNA - single strand DNA; SWCNT – single-walled carbon nanotubes; SWV - square wave voltammetry; TCNQ - 7,7,8,8-tetracyanoquinonedimethane.

The application of the current SPE-MnO_2/MG/BChE biosensor in a real sample assay (like environmental monitoring, safety assessments of food and beverages, etc.) implies an unavoidable presence of interfering agents. The most typical of them is ascorbic acid, which is frequently present in many food-stuffs and is simultaneously the most common electrochemical interfering agent easily oxidized at positive potentials. Other examples of interfering agents commonly found in the environment are ions of heavy metals, like Cd^{2+}, Pb^{2+}, Cu^{2+}, and Co^{2+}.

We examined and confirmed experimentally that interfering agents can have an influence both on the stage of the preincubation with the inhibitor and on the stage of the residual activity assay. The results are summarized in Table S-1. Indeed, the presence of the aforementioned interfering agents in an electrochemical cell considerably influences the electrochemical measuring of the sensor response (see Table S-1). All these effects, however, are insignificant when the concentrations of the interfering agents are lower than 1 μM. In case of ions of heavy metals, threshold values of 1 μM, below which the interfering effect becomes insignificant, are much higher than the levels of maximum permissible (environmentally safe) concentrations that are also given in Table S-1.

As the stage of the preincubation with the inhibitor and the stage of the residual activity assay in our case were carried out separately, the most interesting and important are the effects of the aforementioned interfering agents on the SPE-MnO_2/MG/BChE in the inhibition regime. For this purpose, the relative sensor responses were measured before and after 20-min pre-incubation of a SPE-MnO_2/MG/BChE sensor with the interfering compounds at different concentrations. In contrast to a notable interference of these agents with the electrochemical measuring of the sensor response, only a slight (about 25% or less in the case of Cd^{2+}, and Pb^{2+}) to moderate (about 50% or less in the case of Cu^{2+}, and Co^{2+}) inhibition was found in spite of the extremely high (0.01 - 1 mM) concentrations of the interfering agents. A slight 15% decrease in the relative sensor response was found also for ascorbic acid without any concentration dependence (Table

S-1). Therefore, the presence of the interfering compounds in the analyte apparently does not cause difficulties for performing the quantitative OP inhibitor assay.

These results demonstrate that a SPE-MnO_2/MG/BChE biosensor is a very promising tool for a quantitative cholinesterase inhibitor assay. Moreover, such a high sensitivity contributes to real sample assays that enables performing precision inhibitor analysis in highly diluted real samples with minimized interference from extraneous substances (e.g., ions of heavy metals).

Conclusions

We described a very simple and stable MG/BChE biosensor construct, where BChE is easily accessible both for the substrate and for cholinesterase inhibitors providing their highly sensitive and fast detection in aqueous samples. The herein described example has a specific interest as a promising candidate for the assay of cholinesterase inhibitors that is currently highly required for screening pesticide residues in environmental samples and in food analysis.

Furthermore, it is a promising example of the application of stimuli-responsive microgels as a guest matrix for enzyme immobilization in the field of biosensors. Previously and then here, we demonstrated that through careful control of pH and temperature of the adsorption of stimuli-responsive NIPAM-based microgels with ionic moieties, we can control the amount and the localization of enzymes (BChE in this specific case) interacting with preadsorbed microgels deposited onto graphite surfaces. This outer complexation of BChE with the dangling chains of the microgel rather than an inner penetration into the microgels does not induce any structural deformation/deterioration of the enzyme or steric hindrance to the catalytic sites of BChE. Furthermore, the complex tetrameric BChE structure is placed into a favorable, highly hydrated microenvironment provided by the swollen microgel matrix, which is desirable from the point of stability and activity of the immobilized biomaterial. Being very facile, this new immobilization strategy could be generalized and expanded to design other biosensor systems. It should be noted that an advantageous feature of ionic NIPAM-based microgels is their stimuli-sensitivity along

with the ease of synthesis with broad possibilities to control the mesh size, particle size, charge, and functionalization. Therefore, a perfectly matched pair of microgel/guest species can easily be found on-demand.

Moreover, as one can assure, each stage of surface modification implies deposition of small volumes of specified aqueous solutions onto SPE arrays with following incubations under specified conditions. This technique is applicable for a wide range of sensor surfaces, can be easily automated by means of, e.g., ink-jet printing, and is suitable for large-scale production.

Acknowledgements

This research was supported by the Deutsche Forschungsgemeinschaft within SFB 985 "Functional Microgels und Microgel Systems", the Russian Foundation for Basic Research within RFBR 14-08-01108, the Lomonosov Moscow State University Programm of Development; and the Lomonosov Moscow State University post-genomic programm. L.V.S. and D.V.P. gratefully acknowledge the SFB 985 for financial support of their research stays at the RWTH Aachen University. The authors also acknowledge E.G. Evtushenko for AFM measurements.

Supporting Information. method of SPE modification with MnO_2 nanoparticles, SEM data, AFM data, biosensor manufacturability, effect of interfering compounds measured in different regimes.

References

(1) Briand, J. F.; Jacquet, S.; Bernard, C.; Humbert, J. F. *Vet. Res.* **2003**, *34*, 361-377.

(2) Tayeb, H. O.; Yang, H. D.; Price, B. H.; Tarazi, F. I. *Pharmacol. Ther.* **2012**, *134*, 8-25.

(3) Makhaeva, G. F.; Radchenko, E. V.; Palyulin, V. A.; Rudakova, E. V.; Aksinenko, A. Y.; Sokolov, V. B.; Zefirov, N. S.; Richardson, R. J. *Chem.-Biol. Interact.* **2013**, *203*, 231-237.

(4) Makhaeva, G.; Rudakova, E.; Boltneva, N.; Sigolaeva, L.; Eremenko, A.; Kurochkin, I.; Richardson, R. In *Counteraction to Chemical and Biological Terrorism in East European Countries*, Dishovsky, C.; Pivovarov, A., Eds., 2009, pp 177-194.

(5) Sigolaeva, L.; Makhaeva, G.; Rudakova, E.; Boltneva, N.; Porus, M.; Dubacheva, G.; Eremenko, A.; Kurochkin, I.; Richardson, R. J. *Chem.-Biol. Interact.* **2010**, *187*, 312-317.

(6) Makhaeva, G. F.; Rudakova, E. V.; Sigolaeva, L. V.; Kurochkin, I. N.; Richardson, R. J. *J. Appl. Toxicol.* **2016**, *36*, 1468-1475.

(7) Pundir, C. S.; Chauhan, N. *Anal. Biochem.* **2012**, *429*, 19-31.

(8) Andreescu, S.; Marty, J. L. *Biomol. Eng.* **2006**, *23*, 1-15.

(9) Pohanka, M.; Musilek, K.; Kuca, K. *Curr. Med. Chem.* **2009**, *16*, 1790-1798.

(10) Plamper, F. A.; Richtering, W. *Acc. Chem. Res.* **2017**, *50*, 131-140.

(11) Srinivas, R. L.; Chapin, S. C.; Doyle, P. S. *Anal. Chem.* **2011**, *83*, 9138-9145.

(12) Le Goff, G. C.; Srinivas, R. L.; Hill, W. A.; Doyle, P. S. *Eur. Polym. J.* **2015**, *72*, 386-412.

(13) Zhang, Q. M.; Wang, W. D.; Su, Y. Q.; Hensen, E. J. M.; Serpe, M. J. *Chem. Mater.* **2016**, *28*, 259-265.

(14) Wiese, S.; Spiess, A. C.; Richtering, W. *Angew. Chem.,Int. Ed.* **2013**, *52*, 576-579.

(15) Wiese, S.; Tsvetkova, Y.; Daleiden, N. J. E.; Spiess, A. C.; Richtering, W. *Colloids Surf., A* **2016**, *495*, 193-199.

(16) Such-Sanmartin, G.; Ventura-Espejo, E.; Jensen, O. N. *Anal. Chem.* **2014**, *86*, 1543-1550.

(17) Pich, A.; Richtering, W. In *Advances in Polymer Science*, 2010, pp 1-37.

(18) Wong, Y. M.; Hoshino, Y.; Sudesh, K.; Miura, Y.; Numata, K. *Biomacromolecules* **2015**, *16*, 411-421.

(19) Ogawa, K.; Nakayama, A.; Kokufuta, E. *Langmuir* **2003**, *19*, 3178-3184.

(20) Dubbert, J.; Honold, T.; Pedersen, J. S.; Radulescu, A.; Drechsler, M.; Karg, M.; Richtering, W. *Macromolecules* **2014**, *47*, 8700-8708.

(21) Dubbert, J.; Nothdurft, K.; Karg, M.; Richtering, W. *Macromol. Rapid Commun.* **2015**, *36*, 159-164.

(22) Keerl, M.; Pedersen, J. S.; Richtering, W. *J. Am. Chem. Soc.* **2009**, *131*, 3093-3097.

(23) Schmid, A. J.; Dubbert, J.; Rudov, A. A.; Pedersen, J. S.; Lindner, P.; Karg, M.; Potemkin, I. I.; Richtering, W. *Sci. Rep.* **2016**, *6*.

(24) Buenger, D.; Topuz, F.; Groll, J. *Prog. Polym. Sci.* **2012**, *37*, 1678-1719.

(25) Schild, H. G. *Prog. Polym. Sci.* **1992**, *17*, 163-249.

(26) Pelton, R. *Adv. Colloid Interface Sci.* **2000**, *85*, 1-33.

(27) Khokhlov, A. R.; Starodubtzev, S. G.; Vasilevskaya, V. V. *Adv. Polym. Sci.* **1993**, *109*, 123-175.

(28) Lally, S.; Bird, R.; Freemont, T. J.; Saunders, B. R. *Colloid Polym. Sci.* **2009**, *287*, 335-343.

(29) Pinheiro, J. P.; Moura, L.; Fokkink, R.; Farinha, J. P. S. *Langmuir* **2012**, *28*, 5802-5809.

(30) Sigolaeva, L. V.; Gladyr, S. Y.; Gelissen, A. P. H.; Mergel, O.; Pergushov, D. V.; Kurochkin, I. N.; Plamper, F. A.; Richtering, W. *Biomacromolecules* **2014**, *15*, 3735-3745.

(31) Sigolaeva, L. V.; Mergel, O.; Evtushenko, E. G.; Gladyr, S. Y.; Gelissen, A. P. H.; Pergushov, D. V.; Kurochkin, I. N.; Plamper, F. A.; Richtering, W. *Langmuir* **2015**, *31*, 13029-13039.

(32) Dontsova, E. A.; Zeifman, Y. S.; Budashov, I. A.; Eremenko, A. V.; Kalnov, S. L.; Kurochkin, I. N. *Sens. Actuators, B* **2011**, *159*, 261-270.

(33) Lehmann, S.; Seiffert, S.; Richtering, W. *J. Am. Chem. Soc.* **2012**, *134*, 15963-15969.

(34) Kleinen, J.; Klee, A.; Richtering, W. *Langmuir* **2010**, *26*, 11258-11265.

(35) Eremenko, A. V.; Dontsova, E. A.; Nazarov, A. P.; Evtushenko, E. G.; Amitonov, S. V.; Savilov, S. V.; Martynova, L. F.; Lunin, V. V.; Kurochkin, I. N. *Electroanalysis* **2012**, *24*, 573-580.

(36) Mergel, O.; Gelissen, A. P. H.; Wunnemann, P.; Boker, A.; Simon, U.; Plamper, F. A. *J. Phys. Chem. C* **2014**, *118*, 26199-26211.

(37) Schmidt, S.; Hellweg, T.; von Klitzing, R. *Langmuir* **2008**, *24*, 12595-12602.

(38) Wellert, S.; Hertle, Y.; Richter, M.; Medebach, M.; Magerl, D.; Wang, W.; Deme, B.; Radulescu, A.; Muller-Buschbaum, P.; Hellweg, T.; von Klitzing, R. *Langmuir* **2014**, *30*, 7168-7176.

(39) Ivanov, A.; Evtugyn, G.; Budnikov, H.; Ricci, F.; Moscone, D.; Palleschi, G. *Anal. Bioanal. Chem.* **2003**, *377*, 624-631.

(40) Arduini, F.; Forchielli, M.; Amine, A.; Neagu, D.; Cacciotti, I.; Nanni, F.; Moscone, D.; Palleschi, G. *Microchim. Acta* **2015**, *182*, 643-651.

(41) Shaidarova, L. G.; Ziganshina, S. A.; Medyantseva, E. P.; Budnikov, G. K. *Russ. J. Appl. Chem.* **2004**, *77*, 241-248.

(42) Shaidarova, L. G.; Fomin, A. Y.; Ziganshina, S. A.; Medyantseva, E. P.; Budnikov, G. K. *J. Anal. Chem.* **2002**, *57*, 150-156.

(43) Skladal, P. *Anal. Chim. Acta* **1992**, *269*, 281-287.

(44) Greene, S. *Sittig's Handbook of Pesticides and Agricultural Chemicals, 1st Edition*, 2007, p 1213.

(45) Evtugyn, G. A.; Ivanov, A. N.; Gogol, E. V.; Marty, J. L.; Budnikov, H. C. *Anal. Chim. Acta* **1999**, *385*, 13-21.

(46) Shimomura, T.; Itoh, T.; Sumiya, T.; Mizukami, F.; Ono, M. *Enzyme Microb. Technol.* **2009**, *45*, 443-448.

(47) Somerset, V. S.; Klink, M. J.; Baker, P. G. L.; Iwuoha, E. I. *J. Environ. Sci. Health, Part B* **2007**, *42*, 297-304.

(48) Siriviriyanun, A.; Imae, T.; Nagatani, N. *Anal. Biochem.* **2013**, *443*, 169-171.

(49) Zamfir, L.-G.; Rotariu, L.; Bala, C. *Biosens. Bioelectron.* **2011**, *26*, 3692-3695.

(50) Bonnet, C.; Andreescu, S.; Marty, J. L. *Anal. Chim. Acta* **2003**, *481*, 209-211.

(51) Sun, X.; Zhai, C.; Wang, X. Y. *Bioprocess Biosyst. Eng.* **2013**, *36*, 273-283.

(52) Zhai, C.; Guo, Y. M.; Sun, X.; Zheng, Y. H.; Wang, X. Y. *Enzyme Microb. Technol.* **2014**, *58-59*, 8-13.

(53) Chen, D. F.; Sun, X.; Guo, Y. M.; Qiao, L.; Wang, X. Y. *Bioprocess Biosyst. Eng.* **2015**, *38*, 315-321.

(54) Chauhan, N.; Pundir, C. S. *Electrochim. Acta* **2012**, *67*, 79-86.

(55) Istamboulie, G.; Durbiano, R.; Fournier, D.; Marty, J.-L.; Noguer, T. *Chemosphere* **2010**, *78*, 1-6.

(56) Viswanathan, S.; Radecka, H.; Radecki, J. *Biosens. Bioelectron.* **2009**, *24*, 2772-2777.

(57) Yang, L.; Wang, G. C.; Liu, Y. J.; An, J. J.; Wang, M. *Anal. Bioanal. Chem.* **2013**, *405*, 2545-2552.

(58) Wei, M.; Zeng, G. Y.; Lu, Q. Y. *Microchim. Acta* **2014**, *181*, 121-127.

(59) Liu, Y. J.; Wang, G. C.; Li, C. P.; Zhou, Q.; Wang, M.; Yang, L. *Mater. Sci. Eng., C* **2014**, *35*, 253-258.

TOC Graph

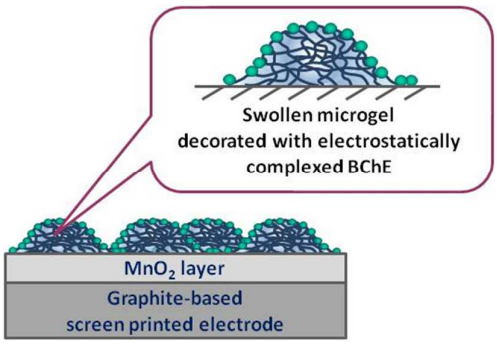
Swollen microgel
decorated with electrostatically
complexed BChE
MnO_2 layer
Graphite-based
screen printed electrode